ELSEVIER

Cement and Concrete Composites **19** (1997) 373–385

0958-9465/97/$17.00

PII:S0958-9465(97)00026-7

Durable Repair of Aged Infrastructures Using Trapping Mechanism of Engineered Cementitious Composites

Yun Mook Lim[a] & Victor C. Li[b]

[a]Applied Mechanics Laboratory, Department of Civil Engineering, College of Engineering, Yonsen University, Seoul (120-749), Korea
[b]Advanced Civil Engineering Material Research Laboratory, Department of Civil and Environmental Engineering, The University of Michigan, Ann Arbor, MI 48109-2125, USA

(Received 23 July 1996; accepted 3 March 1997)

Abstract

This paper introduces the concept of interface crack trapping and demonstrates experimentally the feasibility of this mechanism in a representative repaired concrete system. A microstructurally tailored Engineered Cementitious Composite (ECC) serving as the repair material was found to be most effective in trapping interface cracks such that typical failure modes in repaired systems, such as spalling or delamination, were prevented. It is shown that, for the same geometry and loading conditions, the ECC repair system is stronger, more ductile, more energy absorbing, and shows better crack width control in comparison with controlled systems with concrete or a typical fiber-reinforced concrete repair material. The trapping mechanism and the ECC repair material together represent a novel means to extend the service life of rehabilitated concrete structures. © *1997 Elsevier Science Ltd. All rights reserved.*

Keywords: Engineered Cementitious Composites, trapping mechanism, aged infrastructures.

INTRODUCTION

Most civil engineers and construction industry experts have recognized the deterioration problem of aged infrastructures around the world. For example, 42% of the highway bridges in the USA should be urgently rehabilitated according to FHA (Federal Highway Administration) officials, and the cost of rehabilitation is estimated at $50 billion by the year 2010.[1] The amount and cost for rehabilitation will be much higher if transportation infrastructures such as pavements are included.

The common deterioration of those infrastructures[2] starts from or near the surface. The careful design of overlay or replacement of the deteriorated portion can increase the service life of those infrastructures.[3–5] Many repair materials and techniques have been developed to provide strong, longer lasting rehabilitation.[6] Even with evolving innovative repair materials and techniques, some basic repair problems still remain.[7] In many cases, the repaired infrastructures still fail in the repaired part by spalling or delamination.[8] Those failures usually initiate from the interface, since it is the weakest link in rehabilitated structures.

For durable repair of aged infrastructures, the interface property is considered an important parameter.[2,6] Tensile or shear bond strength is usually accepted as an interface property in practice accompanied by a variety of test techniques.[8] This bond strength may be useful for ranking of repair materials, but is not expected to have field performance predictive capability due to size and geometric effects. On the other hand, interfacial fracture toughness is considered an interface property capable of predicting repair system performance associated with interface crack extension.[6]

In this study, interface fracture mechanics serves as an analytical tool for predicting

whether an interface crack will propagate along the interface (delamination) or will kink-out from the interface, as well as for predicting the load magnitude necessary to drive the crack. If kinking is followed by fracture propagation to the surface of the repair material, then surface spall failure occurs. Both delamination and surface spalling should be prevented for durable rehabilitation. One technique to overcome these failure modes in a repair system is to induce kinking when the system is overloaded, followed by arrest of the kink-crack inside the repair material. We call this the interface crack trapping mechanism. This trapping mechanism can be achieved by applying a well-designed Engineered Cementitious Composite (ECC) as the repair material. The ECC is micromechanically tailored to satisfy the requirement of the trapping mechanism based on interface fracture mechanics.

The objective of this paper is to introduce the trapping mechanism and to report the experimental observations of this mechanism in a representative repair system designed for laboratory-scale test. In the following section, the trapping mechanism theoretical concept is described. Next, the experiments which initially suggest the trapping mechanism are summarized. Experimental details and findings of the representative repair system are provided in the subsequent two sections. It is demonstrated that the interface delamination and the surface spall failure modes can be eliminated by the trapping mechanism attained with a micromechanically designed ECC.

CONCEPT OF TRAPPING MECHANISM

A rehabilitated infrastructure system usually contains a substrate, the repair material, and an interface between these two materials. This is illustrated schematically in Fig. 1 with a bimaterial system loaded in mixed Mode 1 and Mode 2 (indicating Mode I and Mode II in a bimaterial system). The degree of mixity depends on the loading condition and material property contrast between repair and substrate materials. An interfacial flaw can extend along the interface or kink out into the repair/substrate material. For the latter scenario, the interface crack kink condition[9] should be satisfied.

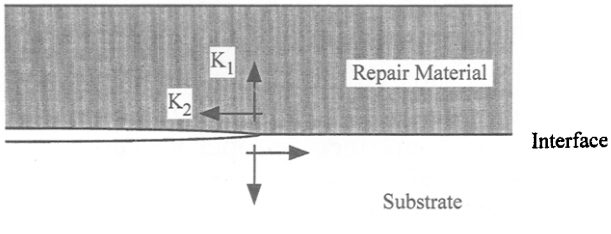

Fig. 1. Typical rehabilitated infrastructure system.

$$\frac{G}{G^t_{max}} < \frac{\Gamma(\hat{\psi})}{\Gamma_c} \tag{1}$$

where G is an energy release rate of the interface crack, and G^t_{max} is a maximum energy release rate at the kinked crack tip. Γ is the interface fracture toughness dependent on phase angles $\hat{\psi}$, and Γ_c is the fracture toughness of the repair material. The phase angle $\hat{\psi}$ represents the mode mixity at the interface crack tip defined as

$$\hat{\psi} = tan^{-1}\left(\frac{K_2}{K_1}\right) \tag{2}$$

where, K_1 and K_2 are the opening mode and the shear mode components (see Fig. 1) of the complex stress intensity factors.[9] Physically, a 0° phase angle means only the opening mode, and 90° phase angle means the pure shear mode. When this interface system is exposed to a certain loading condition, the relative driving force (left-hand side of eqn 1) which is a function of the material mismatch and the phase angle can be analytically calculated. For this calculation, it is assumed that the crack tip behavior is not influenced by boundary conditions and geometry. This assumption is valid for the small K-dominant zone[9] at the interface crack tip. The interface crack tip in this study is expected to satisfy this assumption since there is no aggregate interlocking nor fiber bridging across the interface[6] so that a small process zone relative to other body geometric dimensions is expected.

The relative toughness (right-hand side of eqn 1) should be evaluated from experimentally measured values of the interface toughness and the toughness of the repair material. Γ has been reported for a number of bimaterial systems and is generally found to increase with $\hat{\psi}$.[10,11]

The kinking conditions and possible pattern of interface cracking are illustrated in Fig. 2. If

the relative toughness of a system is greater than the relative driving force for all phase angles, an interface crack always kinks out from the interface according to the kink condition (Pattern I). On the other hand, if the relative toughness is always less than the relative driving force, no kinking can occur (Pattern III).

Patterns II-1 and -2, which show in-plane propagation or kinking of the interface crack depending on the phase angle, are different from the previous two extreme cases. For example, the interface crack has a tendency to kink out when the phase angle is larger than a certain phase angle (30° in Pattern II-1). However, the interface crack will propagate along the interface when the phase angle is less than 30°.

When an interface crack propagates along the interface, it may have a brittle behavior because there is no bridging or interlocking along the interface. On the other hand, when an interface crack kinks out from the interface, it can show two different cracking behaviors depending on the fracture resistance of the repair material. If the repair material is brittle, the kinked crack cannot be stopped in the repair material and forms a surface spall. On the contrary, if the repair material has rapidly rising fracture resistance, the kinked crack can be stopped or 'trapped' in the repair material. There is no more crack propagation when the driving force of the kinked crack equals the increasing fracture resistance of the repair material. This is possible if the repair material possesses an *R*-curve characteristic, such as that due to fiber bridging across a matrix crack (Fig. 3) if the repair material is fiber reinforced.

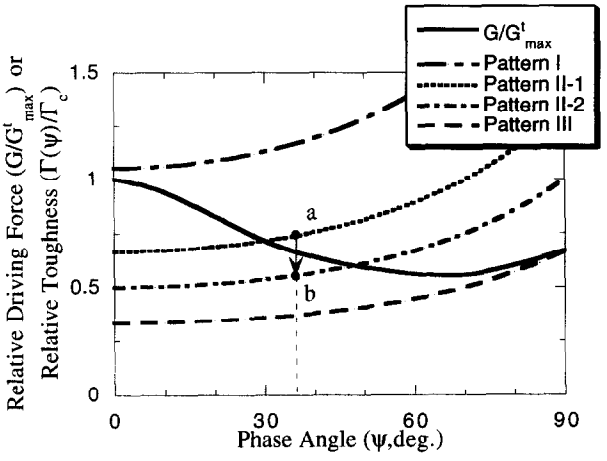

Fig. 2. Possible pattern of interface cracking behavior.

This kinking and trapping mechanism can be further explained using Patterns II-1 and -2 in Fig. 2. For a repair material with low initial toughness, an interface crack can kink out from the interface with a certain phase angle (Pattern II-1, a). Subsequent rise in fracture resistance Γ_c according to the *R*-curve behavior of the repair material can lead to a drop in $\Gamma(\hat{\psi})/\Gamma_c$. In this process, the relative toughness curve should be moved downward (Pattern II-1 to Pattern II-2 in Fig. 2), so that eqn 1 is violated. At this point, the actual toughness of the damaged repair material is tougher than that of the undamaged repair material and the kinked crack is trapped in the repair material. Further loading causes the mother crack to propagate again along the interface, because the kink condition is changed from 'a (kinked cracking)' to 'b (interface cracking)' in Fig. 2. When the crack tip has escaped from the influence of the

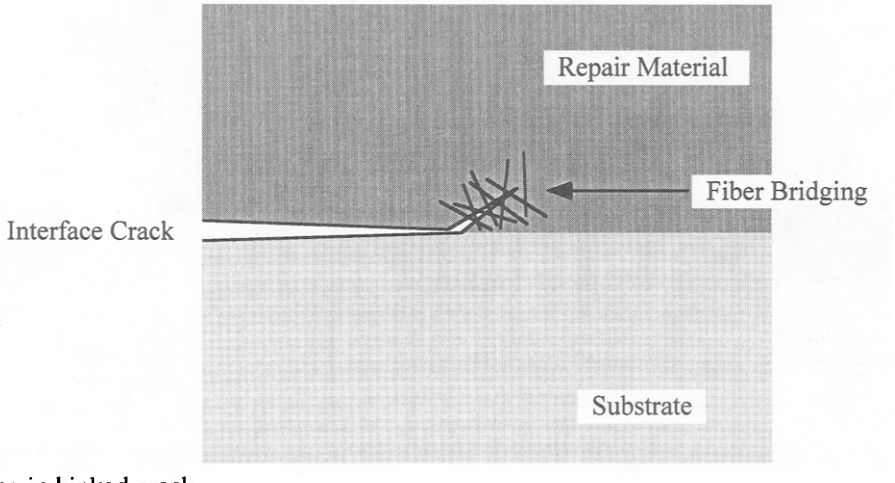

Fig. 3. Fiber bridging in kinked crack.

first damaged zone, the relative toughness curve moved upward again (Pattern II-2 to Pattern II-1), and the propagated interface crack kinks out from the interface again. Thus, the sequence of kinking, damaging, trapping, and interface propagation as described above will be repeated under continued increasing load until the full interface is exhausted or other failure modes take over.

In Fig. 4, the conceptual trapping mechanism with load–displacement relation is illustrated. This failure process involves a large amount of energy absorption associated with extensive subsurface damage in the repair material without loss of load carrying capacity of the repaired system. The interface crack trapping mechanism described here can be exploited in a repair system to provide more durable rehabilitated infrastructures.

DISCOVERY OF THE TRAPPING MECHANISM

In the previous section, the concept of an interface crack trapping mechanism was introduced. This concept was motivated by theoretical considerations and experimental observations in a series of tests to evaluate the interfacial toughness of various potential repair materials.[6] Among plain concrete, fiber reinforced concrete (FRC), and ECC, the ECC was found to produce the special characteristics of trapping described. Some pertinent results of that test are summarized in this section.

The specimens and loading configuration are illustrated in Fig. 5. The phase angle $\hat{\psi}$ is a function of s in Fig. 5 and of material property mismatch.[12] In the experiment, therefore, $\hat{\psi}$ is varied by moving the specimens with respect to the fixed load and support points.

ECC is a special type of fiber reinforced cementitious composite microstructurally tailored according to micromechanical principles.[13] This results in a deliberate combination of fiber, matrix and interface properties which leads to a composite showing tensile strain-hardening with strain capacity of as much as 6%. ECC is extremely damage-tolerant, exhibiting a high degree of fracture resistance[14] with toughness around 25 kJ/m^2. The material reveals an R-curve type behavior (Fig. 6) with a high tear modulus[16] rising from a low initial toughness of 20 J/m^2. This is exactly

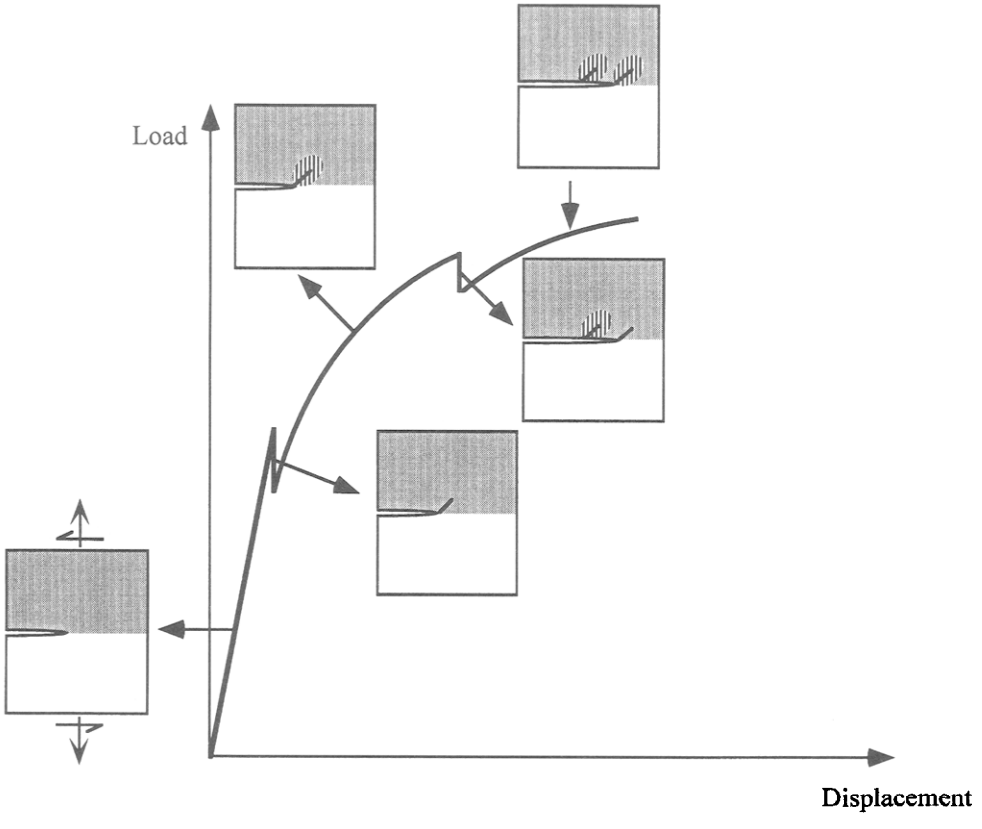

Fig. 4. Trapping mechanism in a bimaterial interface system.

the type of material behavior most suitable for initiating and then trapping the kink crack in the repair material. The composition of the ECC used in this test series can be found in Table 1. Compared with ordinary FRC, ECC has relatively lower matrix toughness and strong fiber bridging. More details on ECC can be found in Li.[13]

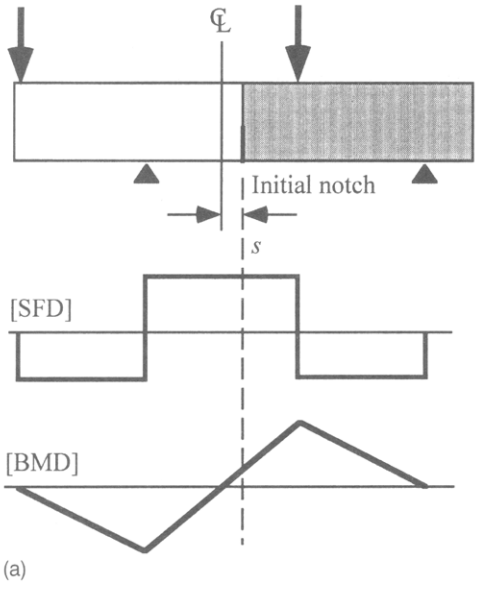

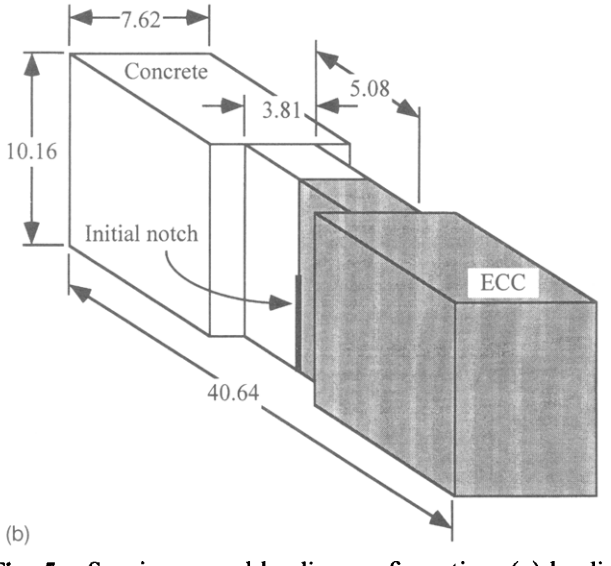

Fig. 5. Specimens and loading configuration: (a) loading configuration and bending moment/shear force diagram; (b) dimension of interface specimen (unit: cm).

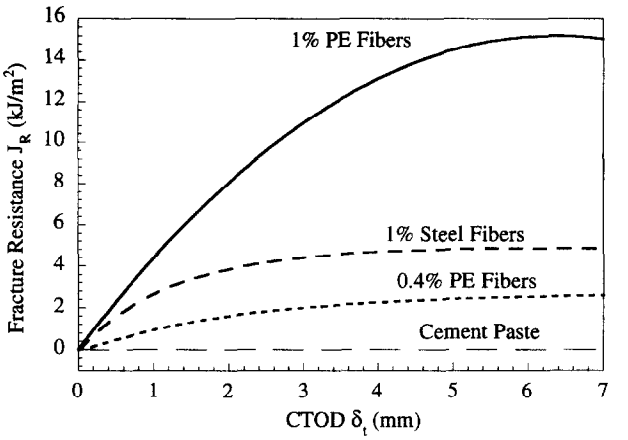

Fig. 6. Fracture resistance behavior in some composites (Li *et al.*).[15]

Figure 7 plots the experimentally determined interface toughness of the concrete/ECC system as a function of phase angle. The calibration for this interface specimen was developed based on finite element analysis assuming linear elastic material behavior.[12] There is only one data point at the phase angle 60° because of the increasing difficulty of the test at high phase angles when other failure modes (such as bending failure away from the bimaterial interface plane) dominate.

At lower phase angles ($<41°$), the initial notch propagates along the interface and there is no kinking behavior. On the contrary, at higher phase angles ($>41°$), the initial notch propagates along the interface slightly (about 0–2 mm from the notch tip) and then kinks out from the interface. This behavior can be explained using the kinking condition illustrated in Fig. 8. In Fig. 8, the analytically evaluated relative driving force[9] is also shown. For the relative toughness, the curve fit based on a model of Evans & Hutchinson[17] to experimental data for the interface toughness (Fig. 7), and an initial toughness of $\Gamma_c = 14$ J/m^2 at 14 days age (estimated at 70% of 20 J/m^2 mea-

Table 1. Material composition

Material	*Cement*	*Water*	*FA*	*CA*	*SF*	*SP*	*Fiber vol. fraction*
Concrete	1.0	0.5	2.27	1.8	—	—	—
SFRC	1.0	0.5	2.27	1.8	—	—	0.01
ECC	1.0	0.35	0.5	—	0.1	0.01	0.02

FA: fine aggregate; CA: coarse aggregate (maximum size <9.5 mm); SF: silica fume; SP: superplasticizer.

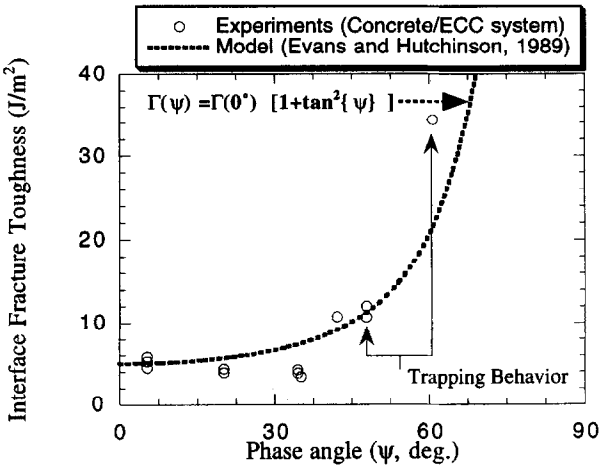

Fig. 7. Interface fracture toughness.

sured at 28 days age) was used. Comparison between the relative crack driving force and the relative toughness indicates that kinking should be expected at a phase angle higher than 41° for the concrete/ECC bimaterial system.

Figure 9 shows kinked and trapped cracks for a specimen tested with $\hat{\psi} = 60°$. The trends of measured load–deflection curves shown in Fig. 10(a,b) well matched the expected behavior illustrated in Fig. 4. The first load drop might be related to the slight propagation of interface crack and the first kinked crack. Thus, the first load drop in the trapping cases (the phase angle $> 41°$) was used to calculate the interface fracture toughness.

In this specimen, the final failures may have occurred due to the limited size of the specimens. The specimens tested at the phase angle 47° (Fig. 10(a)) failed due to bending in the concrete part after several small kinked cracks trapped in the ECC material. The specimen

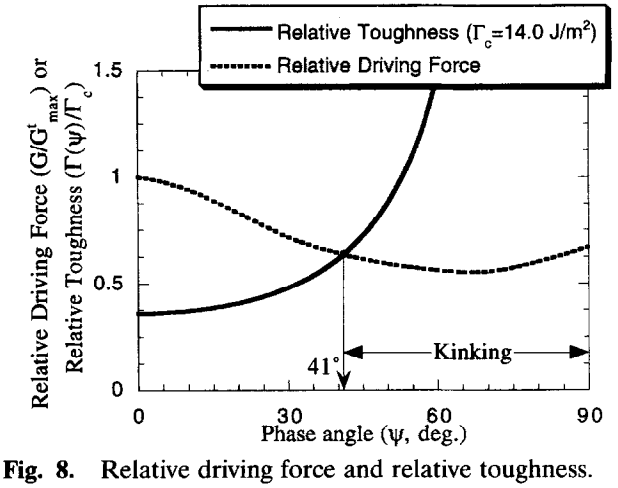

Fig. 8. Relative driving force and relative toughness.

tested at the phase angle 60° (Fig. 10(b)) was designed to prevent such bending failures. This specimen failed due to an interface crack which started from the top of the specimen after the second kinked crack was trapped in the ECC material. If the specimens were larger and not constrained by boundary conditions, the trapping mechanism might be repeated successively.

To test this hypothesis, and to further investigate the trapping mechanism as a means to prolong the durability of the repair system by resisting delamination and spalling failure, a new series of experiments was designed. This new series utilized specimens more representative of an actual repair system — bonded overlay of a concrete pavement above a joint. This experimental investigation is described in the following section.

EXPERIMENTAL PROGRAM

Overlay is usually applied as a surface rehabilitation on deteriorated pavements, bridge decks,

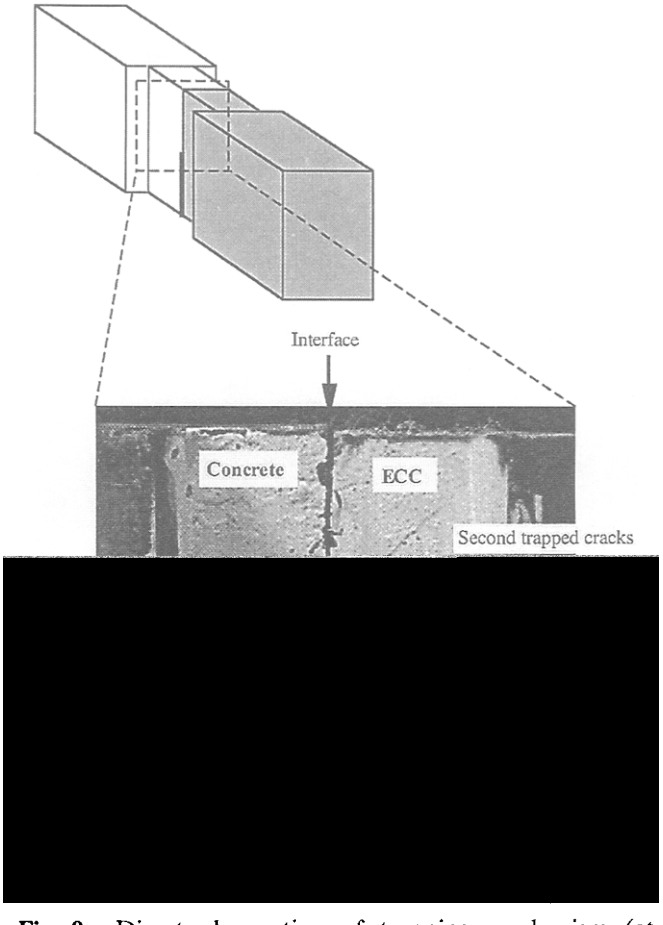

Fig. 9. Direct observation of trapping mechanism (at phase angle of 60°).

parking lots and industrial floors for riding quality or strengthening of structures.[2] These deteriorated infrastructures might contain cracks or joints, and these defects could be the initiation points of failures in rehabilitated systems. Reflective cracking in the repair material above a joint in the original pavement is a commonly observed phenomenon of overlay failure. Figure 11 shows a schematic of a specimen designed to simulate such a repaired system.

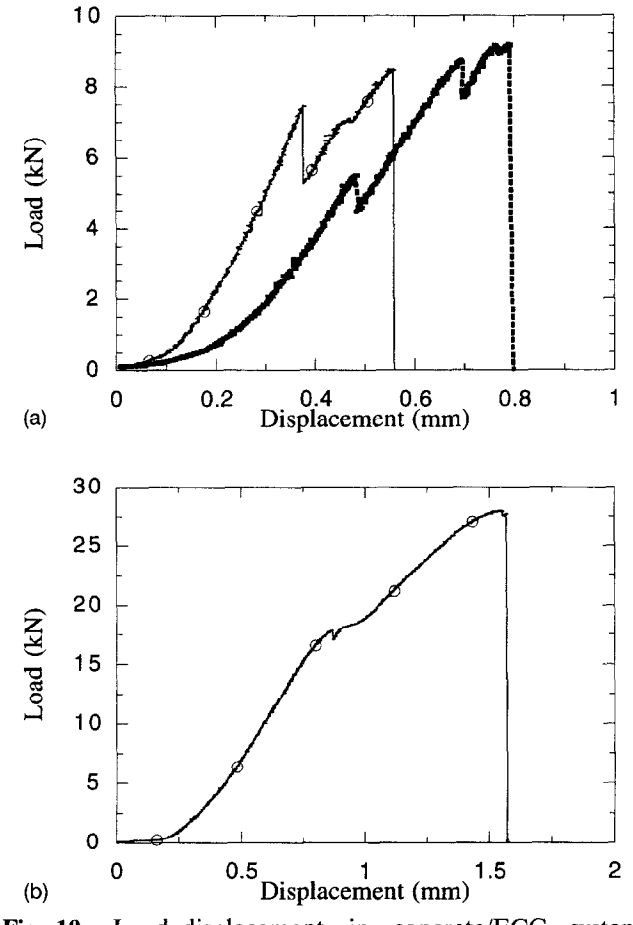

Fig. 10. Load–displacement in concrete/ECC system with trapping behavior: (a) load–displacement behavior at phase angle of 47°; (b) load–displacement behavior at phase angle of 60°.

Specimen and loading condition

The specimens in this experiment were designed to include a defect in the form of an interfacial crack between the repair material and the concrete substrate, as well as a joint in the substrate. The dimensions of the designed specimen and the loading configuration are illustrated in Fig. 11. Four-point bend loading was selected as a general loading condition. The specimen was tested upside down to minimize the effect of gravity load at the initial notch tips.

This loading configuration can provide a stable interface crack propagation condition, when the crack propagates along the interface.[18] The specimen shape and loading condition also coincide with those used for the measurement of interface fracture toughness at phase angles about 41–45°. This is the approximate phase angle regime (Fig. 8) when the kinking condition for the concrete/ECC interface crack is satisfied.

An MTS-810 close-loop machine with Test Star digital control system was used for load application. Load and machine displacement were measured. The loading rate in this test was 0.005 mm/s for quasi-static loading.

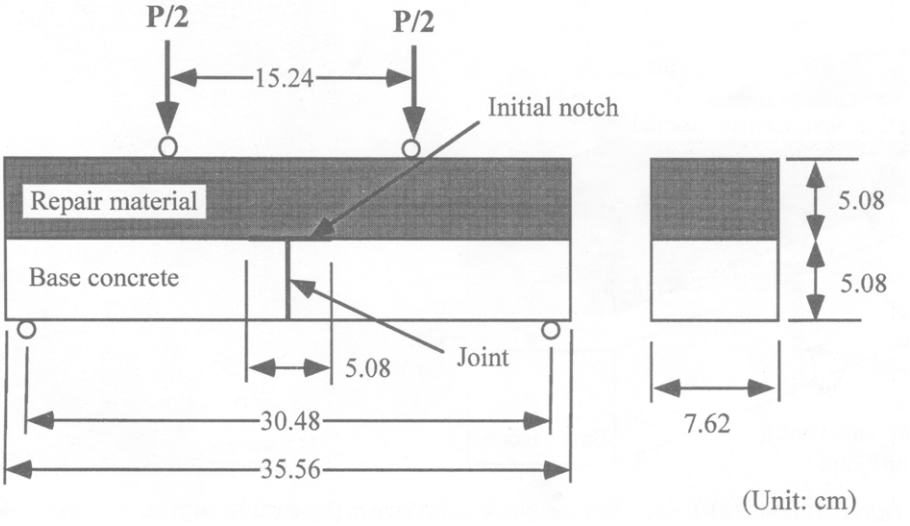

Fig. 11. Dimension of specimen and loading configuration for overlay system.

Material

In this study, three different materials were used as repair materials — concrete, steel fiber reinforced concrete (SFRC) and ECC. Concrete and SFRC have been used as repair materials in the construction industry. The behavior of overlay systems using these two materials as controls was compared with the overlay system behavior using ECC as a potential repair material. The material compositions are tabulated in Table 1.

Crushed limestone with 9.5 mm maximum size was used as coarse aggregate, and ordinary river sand was used as fine aggregate for the concrete and SFRC mix designs. Standard 50–70 silica sand was used for the fine aggregate for ECC. The dimensions of the steel fiber for SFRC were 30 mm in length and 500 μm in diameter (ZL 30/50 fiber) with hooked ends. Spectra fiber (high modulus polyethylene), with 12.7 mm in length and 28 μm in diameter, was used for ECC.

An Omni mixer was used for the mixing of these materials with 4 min. mixing before adding fiber and 4 min. mixing with fibers (only 4 min. for the concrete case).

Specimen preparation

The base concrete blocks were cast (see Fig. 12(a)) and demolded at 24 h age after casting. This concrete was cured under water for 4 weeks, and then dried for 1 week in laboratory air. These concrete blocks were cut into four small blocks using a diamond saw, 24 h before the second casting with repair materials (see Fig. 12(b)). In the second casting, a repair material was cast against the cut surface of the substrate concrete blocks. This cut surface provides the same surface condition of the substrate for each of the two specimens in each overlay system. The initial notch and joint were made by applying a smooth tape on the substrate blocks (see Fig. 12(c)) prior to casting the overlay repair materials.

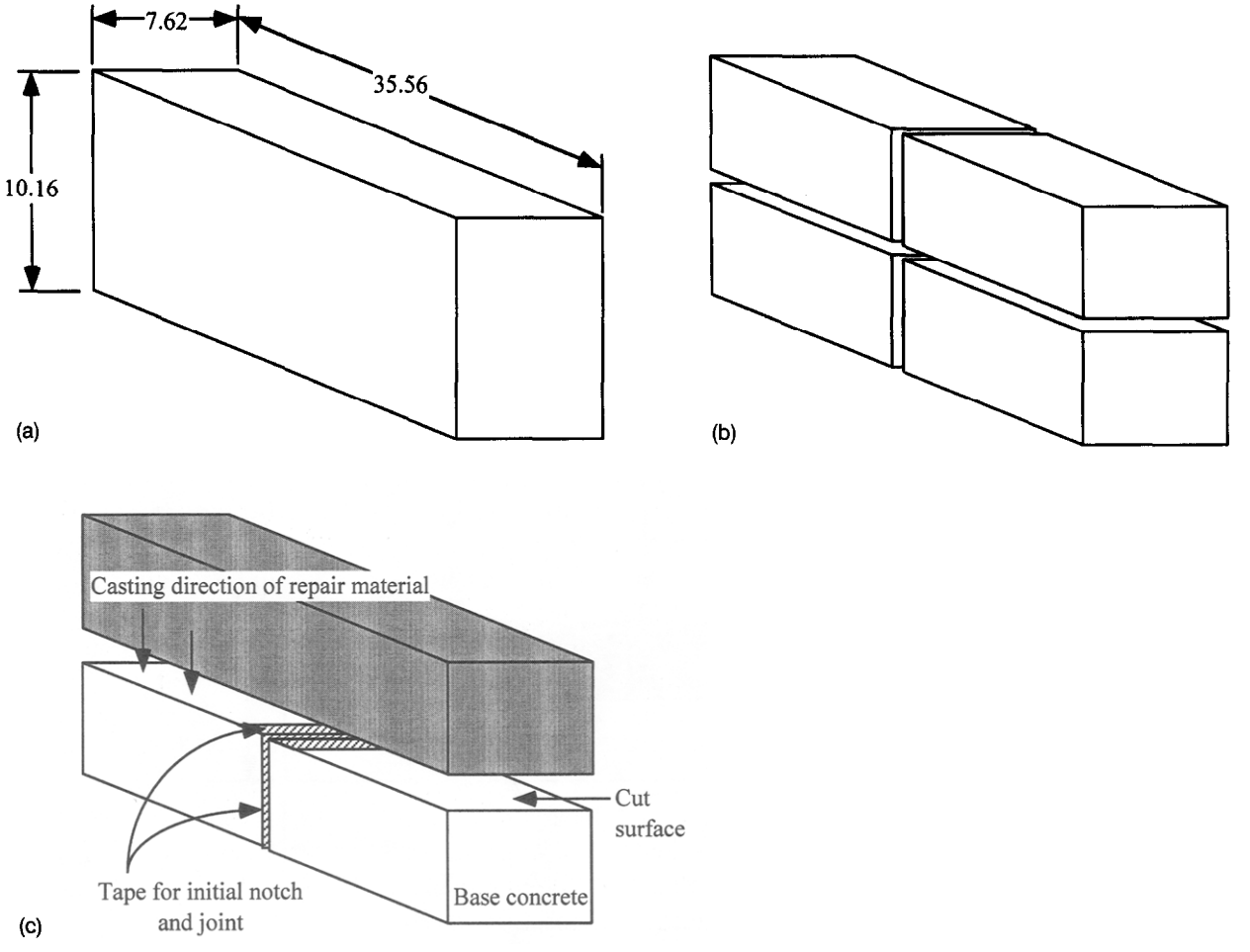

Fig. 12. Specimen preparation: (a) base concrete block (unit: cm); (b) cutting of base concrete block; (c) casting with repair materials.

Table 2. Material properties

Material	Elastic modulus (GPa)	MOR[a] (MPa)
Base concrete	25.8	4.6
Repair concrete	24.9	4.6
SFRC	26.1	10.9
ECC	18.0	13.9

[a] 28 days testing results.

In the second casting, the specimens were demolded after 48 h, and subsequently cured for 2 weeks under water. The reason to wait 48 h before demolding is that the interface specimens are usually fragile, especially at an early age. During the 48 h before demolding, water was constantly sprayed onto the specimens to avoid shrinkage cracking in the repair material and interface.

Thus, the base concrete was cured for a total of 7 weeks (6 weeks water curing plus 1 week drying curing), and the repair materials were cured for 2 weeks under water. The specimens were dried for 24 h before the testing. Two specimens for each overlay system were tested.

The material properties of the base concrete and the repair materials are reported in Table 2. The base concrete mix design is similar to the mixes used in the construction of rigid pavements, with a minimum compressive strength of 24 MPa and flexural strength of 4.5 MPa. The tested flexural strength of base concrete at 28 days was 4.6 MPa. The elastic modulus of each material was measured directly from compressive stress–strain curves for each material. Two strain gages were attached on a compression cylinder specimen 7.62 cm in diameter and 15.24 cm in height. The reported values are the average of three tests for each material.

EXPERIMENTAL RESULTS AND DISCUSSION

The overall load–deflection behaviors in the three different overlay systems are illustrated in Fig. 13. In the ECC overlay system, the ultimate load is approximately 2 to 2.5 times larger than that of the concrete overlay system, and 1 to 1.25 times larger than that of the SFRC overlay system. For the deflection at peak load, a reflection of the system ductility and energy absorption capacity, the ECC overlay system is 3.5 to 6 times larger than the SFRC overlay

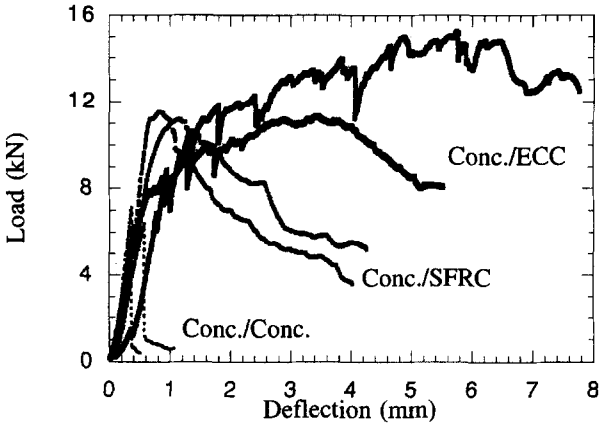

Fig. 13. Load–deflection behavior in overlay systems.

system and 8.75 to 15 times larger than the concrete overlay system.

In many cases, the deformation capacity might be more important than the strength. The causes of failure in many infrastructures might be excessive uneven deflection in structures or imposed straining. The superior deflection capacity of the ECC overlay system can provide good serviceability without any major failure.

In addition, the energy absorption capacity in the ECC overlay system is tremendously improved when it is compared with the other systems. The area under the load–deflection curve of the ECC overlay system is about two to four times larger than that of the SFRC overlay system, and 35 to 107 times larger than that of the concrete overlay system. This remarkable improvement of energy absorption capacity in the ECC overlay system can contribute to the integrity of rehabilitated infrastructures subjected to impact or other high energy input load.

The first load drop due to interface crack propagation can be estimated using the interface fracture toughness of the concrete/ECC interface system. The phase angle of the tested overlay system is 43°, and the interface toughness (from Fig. 7) is estimated at 9.8 J/m^2. Using these values, the load at the first interface crack propagation should be approximately 4.6 kN.[18] According to the testing result in the ECC overlay system, the first interface crack propagation occurred at about 6.5 kN. The 40% difference may be a result of differences in specimen preparation (different cutting or casting directions).

A typical damaged appearance for each overlay system is shown in Fig. 14. In the concrete

overlay system, one tip of the interface crack propagated along the interface for about 5 mm and then the crack kinked out to concrete (repair material) with a sudden load drop. The fractured halves of the specimens separated completely. In the SFRC overlay system, the interface crack kinked out from the initial notch tip on the interface into the SFRC and the load decreased gradually. The fractured halves remained attached by the bridging fibers.

In the ECC overlay systems, several kinking and trapping behaviors are observed. These are through-thickness propagations, and interface and kink crack extensions can be seen on both front and back sides of the specimens. The sequence of cracking behavior for one of the two ECC overlay systems tested is illustrated in Fig. 15. The arrows and the numbers beside the arrows indicate the direction of crack propagation and the sequence of cracking. The roman numerals in circles are the sequence of the kinked cracks and the flexural crack development. The right-hand side of the initial notch propagated slightly along the interface about 2 mm (1), and the crack kinked out from the interface (2). After the first kinked crack propagated upward about 20 mm, the kinked crack was stopped in the ECC. Then under increasing load, the mother crack propagated again along the interface about 27 mm (3), and the crack kinked out from the interface into the ECC (4). This was the second kinked crack, and the load was still increased. The third kinked crack then developed from the initial notch tip on the left-hand side (5), and it was again trapped in the ECC material. The fourth and fifth cracks

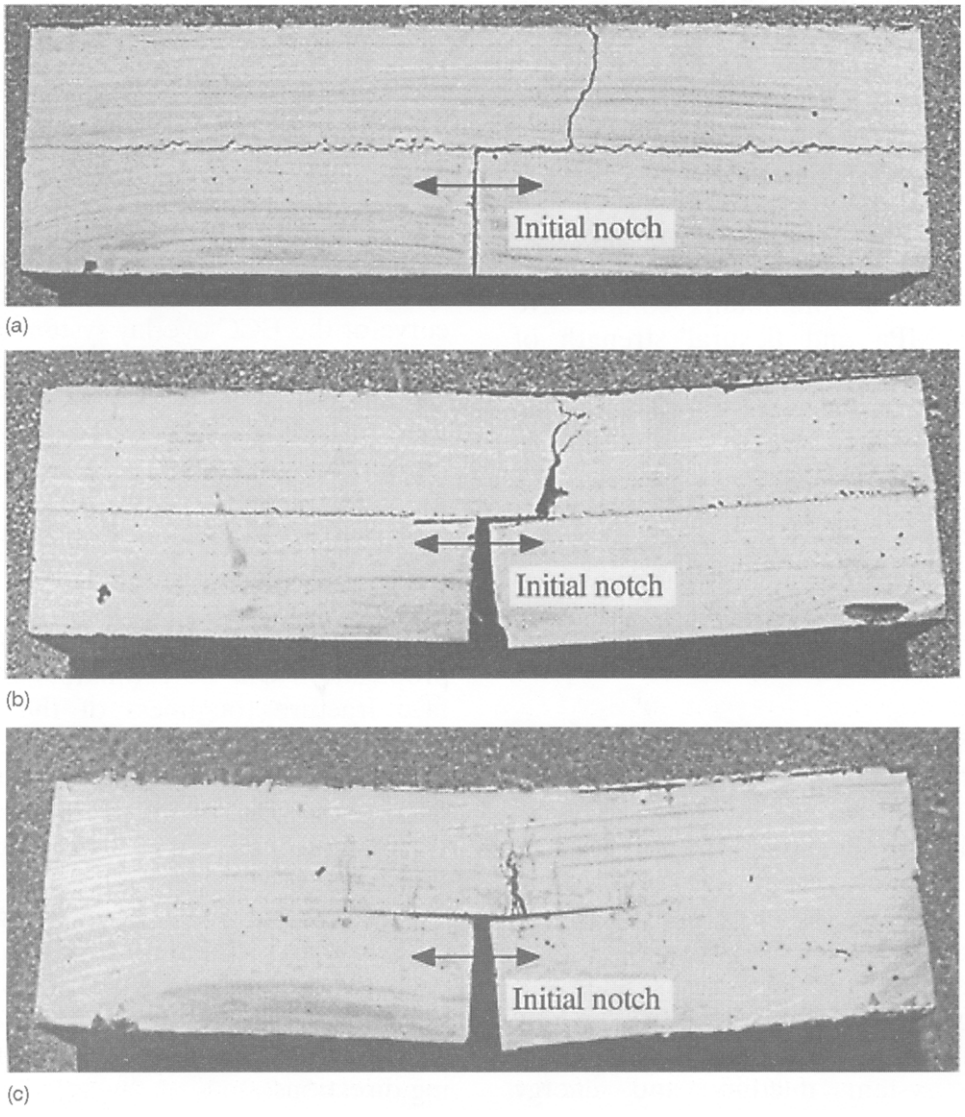

Fig. 14. Cracking in overlay systems: (a) concrete overlay system (assembled after test); (b) SFRC overlay system; (c) ECC overlay system.

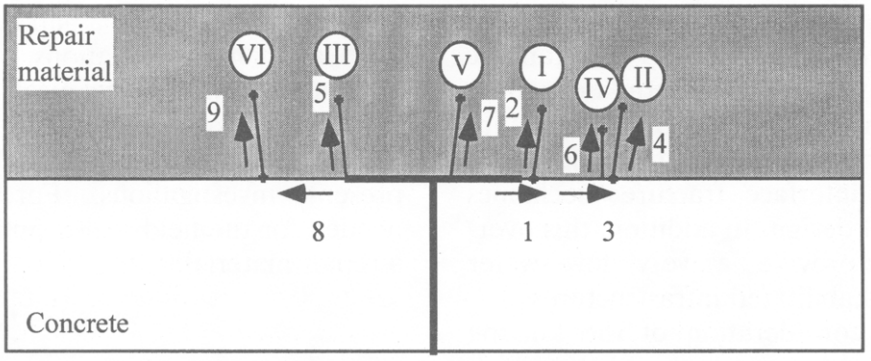

Fig. 15. Kinked cracks development in ECC overlay system.

developed at very near the second kinked crack (6) and almost in the middle of the specimen (7) respectively. The fifth crack might have developed due to flexural loading. At the same time, the mother crack on the left-hand side propagated along the interface about 23 mm (8), and the sixth crack kinked out to the ECC (9). Then, several microcracks were developed around the kinked cracks and flexural crack with load increments. The final failure of the ECC overlay system was the opening of the fifth crack. The flexural stress at failure is estimated at 13.0 to 17.3 MPa, treating the ECC overlay as a free beam without the concrete substrate. This failure stress is comparable with the flexural strength ($\sim$13.9 MPa) of ECC, further supporting the hypothesis of a flexural failure mode in the ECC overlay repair system.

The most significant differences in external appearance after testing between the ECC overlay system and the other overlay systems are the number of cracks and the crack width. Only one macrocrack at one side of the initial notch in the overlay systems is found in the concrete and the SFRC overlay systems, and this crack opening is the final failure of the concrete and the SFRC overlay systems. However, in the ECC overlay system, small kinked cracks are sequentially developed on both sides of the initial notch, increasing with the deflection of specimens. This means that the ECC overlay system was able to redistribute the load and utilize more material to resist the final failure.

The pattern of kinked cracks is different in the ECC overlay system compared with that of the interface toughness test specimen (Fig. 9 and Fig. 14(c)) because of the stress field difference in the ECC associated with different loading and geometry configurations in the two specimens.

Also, the crack width in the ECC overlay system (about 20–40 μm) is much smaller than the other overlay systems (sub-millimeter for SFRC) at the peak load. This is one of the outstanding characteristics of ECCs.[19] The crack width is a very important parameter in infrastructures because the crack width is related to the water flow rate,[20] which was found to scale with the third power of crack width.[21] One order of magnitude in crack width reduction can decrease three orders of magnitude in water penetration rate into the structures. This large reduction of water penetration can dramatically lower corrosion rate of rebars in rehabilitated reinforced concrete structures, and minimize the disturbance of bases under an overlaid pavement. Thus, the reduction of crack width in the ECC overlays can directly provide a longer life of rehabilitated infrastructures.

CONCLUSIONS

The concept of an interface crack trapping mechanism in a bimaterial system is introduced. This trapping mechanism is confirmed in experimental investigations involving specimens resembling bonded pavement overlay system. The trapping behavior cannot be found in the other overlay systems (the concrete and the SFRC overlay systems) tested.

The ECC overlay system with trapping mechanism can prevent the most common failures in rehabilitated infrastructures, such as spalling and delamination of repair parts. Also, high ultimate strength and large deflection capacity with large amount of energy absorption can be expected. The ultimate failure mode has been shifted from one associated with interface crack

extension to one associated with the flexural strength of the repair material. This dramatic improvement in terms of strength, deflection, energy absorption capacity and ultimate failure mode is not feasible without the trapping mechanism based on interface fracture mechanics and ECC material design. In addition, this overlay system can provide a very low water permeability in rehabilitated infrastructures.

Based on the consideration of the kinking condition expressed by eqn 1, the SFRC which also possesses *R*-curve fracture characteristics should lead to crack trapping. However, the experiments show that the SFRC specimens failed by a single kink-out crack which was not trapped, although a more gradual load descending branch was observed compared with the test result of the concrete/concrete system. This is likely due to either a slow rise in the *R*-curve, so that while Γ_c increases with kinked crack length, eqn 1 was never violated before the kink crack reached the free surface of the overlay. In contrast, the ECC with a rapidly rising *R*-curve forces the crack back into the interface under continued rising load by reducing the ratio of $\Gamma(\hat{\psi})/\Gamma_c$ rapidly. In addition, crack kinking is greatly enhanced due to the low initial toughness of the ECC such that repeated kink-trapping rather than delamination is guaranteed.

The observed crack pattern may also be alternatively interpreted as a result of the strain-hardening characteristics of the ECC overlay. The high (at about 45° and turning almost in a horizontal direction within a few millimeters, as determined by FEM analysis) tensile stress near the interface crack tip causes the ECC to go into strain-hardening, and to accommodate the local stress with microcrack inelastic deformation. In this case, the interface crack never kinks out, but is trapped inside the interface due to an effectively toughened interface. This interpretation implies an interface with *R*-curve behavior. The damage in the ECC becomes part of the interfacial behavior. For either interpretation of trapping in interface or in the ECC, improvement in mechanical performance is unequivocally demonstrated to exist in the concrete/ECC repair system.

Thus, the repair system with ECC trapping mechanism can achieve durable rehabilitation in aged infrastructures. This newly developed technique can present a new direction of design and selection of materials for durable rehabilitation. However, there is still a gap between laboratory test and field situations. Specifically, the environmental or mechanical loading condition and geometry of repair can be much more complex than the idealized tests conducted in the present investigations. Further studies are needed for the field-scale application of ECC as a repair material.

ACKNOWLEDGEMENTS

Helpful discussions with Professor Michael Thouless on interface mechanics are gratefully acknowledged. This research has been partly funded by a grant from the National Science Foundation to the University of Michigan (NSF-G-CMS-9601262).

REFERENCES

1. Ashley, S., Bridging the cost gap with composites. *Mech. Eng.*, **118** (1996) 76–80.
2. Deming, B. M., Aktan, H. & Usmen, M., Test for polymer overlay interface on concrete. In *Third Materials Engineering Conference 1994, Infrastructure: New Materials and Methods of Repair*, ed. K.D. Basham. ASCE, San Diego, CA, pp. 709–715.
3. Sprinkel, M. M., Polymer concrete bridge overlays. In *International Congress on Polymers in Concrete 1991*, ACI, Detroit, MI.
4. Krauss, P. D., Bridge deck repair using polymer. In *International Congress on Polymer Concrete 1991*, ACI, Detroit, MI.
5. Fontana, J. J. & Bartholomew, J., Use of concrete polymer materials in the transportation industry. In *Application of Polymer Concrete 1981*, ACI, Detroit, MI, pp. 23–31.
6. Li, V. C., Lim, Y. M., & Foremsky, D. J., Interfacial fracture toughness of concrete repair materials. In FRAMCOS-2 1995, *Fracture Mechanics of Concrete Structures*, ed. F. H. Wittmann. AEDIFICATIO Publishers, Zurich, Switzerland, pp. 1329–1344.
7. Warner, J., Even with innovative materials, the basic still matter. In *Third Materials Engineering Conference 1994, Infrastructures: New Materials and Methods of Repair*, ed. K. D. Basham. ASCE, San Diego, CA, pp. 72–79.
8. Emmons, P. H., *Concrete Repair and Maintenance Illustrated*. Concrete Publishers & Consultants, Kingston, 1994.
9. Hutchinson, J. W. & Suo, Z., Mixed mode cracking in layered materials. *Adv. Appl. Mech.*, **29** (1992) 63–191.
10. Cao, H. C. & Evans, A. G., An experimental study of the fracture resistance of bimaterial interface. *Mech. Mater.*, **7** (1989) 295–304.
11. Evans, A. G., Rühle, M., Dalgleish, B. J. & Charalambides, P. G., The fracture energy of bimaterial interfaces. *Mater. Sci. Eng. A*, **126** (1990) 53–64.
12. O'Dowd, N. P., Shih, C. F. & Stout, M. G., Testing geometry for measuring interfacial fracture toughness. *Int. J. Solids Struct.*, **29** (1992) 571–589.

13. Li, V. C., From micromechanics to structural engineering — the design of cementitious composites for civil engineering applications. *JSCE J. Struct. Mech. Earthquake Eng.*, **10**(2), (1993) 37–48.
14. Li, V. C. & Hashida, T., Engineering ductile fracture in brittle matrix composites. *J. Mater. Sci. Lett.*, **12** (1993) 898–901.
15. Li, V. C., Maalej, M. & Lim, Y. M., Fracture and flexural behavior in strain-hardening cementitious composites. In *Fracture of Brittle Disordered Materials: Concrete, Rock and Ceramics 1995*, eds G. Baker & B. L. Karihaloo. E&FN Spon, London, pp. 101–115.
16. Maalej, M., Fracture resistance of engineered fiber cementitious composites and implications to structural behavior. Ph.D. thesis, University of Michigan, Ann Arbor, 1994.
17. Evans, A. G. & Hutchinson, J. W., Effects of non-planarity on the mixed mode fracture resistance of bimaterial interfaces. *Acta Metall.*, **37** (1989) 909–916.
18. Charalambides, P. G., Lund, J., Evans, A. G. & McMeeking, R. M., A test specimen for determining the fracture resistance of bimaterial interfaces. *J. Appl. Mech.*, **56** (1989) 77–82.
19. Li, V. C., Mihashi, H., Wu, H. C., Alwan, J., Brincker, R., Horii, H., Leung, C., Maalej, M. & Stang, H., Micromechanical models of mechanical response of HPFRCC. In *High Performance Fiber Reinforced Cementitious Composites*, Rilem Proceedings 31, 1996, eds A.E. Naaman & H.W. Reinhardt, pp. 43–100.
20. Wu, H. C., Lim, Y. M. & Li, V. C., Shrinkage behavior of cementitious composites with recycled fiber. In *Proceedings of the 2nd Annual Great Lakes Geotechnical/Geoenvironmental Conference 1994*, Purdue University, Lafayette, pp. 155–166.
21. Tsukamoto, T., Tightness of fiber concrete. *Darmstadt Concrete*, **5** (1990) 215–225.